

**Airborne
Spectral
Photometric
Environmental
Collection
Technology**

**ASPECT Response to
East Palestine Derailment, East Palestine, Ohio
7 February 2023**



ASPECT Mission Supporting:
Region 5 On-Scene Coordinator

ASPECT TEAM

Paige Delgado
Project Officer/Planning Support
Delgado.Paige@epa.gov
469-371-2529

Jill Taylor
Chemical/Photometric Lead
Taylor.Jillianne@epa.gov
214-406-9896

Charles Miller
Miller.Charles.T@epa.gov

Contents

| | |
|---------------------------------------------------------------|-----------|
| Acronyms and Abbreviations | 3 |
| Executive Summary | 4 |
| Overall, Mission and Collection Design | 4 |
| Data Results | 5 |
| Conclusion | 13 |
| Appendix A - Table 1. ASPECT Automated Compounds | 16 |
| Appendix B. ASPECT Sensor System Description | 19 |

Acronyms and Abbreviations

| | |
|---------|---------------------------------------------------------|
| Alt | Altitude (in feet) |
| AGL | Above Ground Level |
| cm | centimeter |
| CST | Central Standard Time |
| DEM | Digital Elevation Model |
| Digital | Digital photography file from the Nikon D2X camera |
| ft | feet |
| FTIR | Fourier Transform Infrared Spectrometer |
| igm | Spectral data format based on grams format |
| IR | Infrared |
| IRLS | Infrared Line Scanner |
| jpg | JPEG image format |
| kts | knots |
| mph | miles per hour |
| m/s | meters per second |
| MSIC | Digital photography file from the Imperx mapping camera |
| MSL | Mean Sea Level Altitude (in feet) |
| ppm | parts per million |
| UTC | Universal Time Coordinated |

Executive Summary

On 3 February 2023 at approximately 2100 EST a Norfolk Southern freight train derailed and caught fire just east of East Palestine, OH. Information provided by the railroad indicated that 100-plus of railcars contained hazardous materials including vinyl chloride and propylene. Local authorities issued a downwind evacuation order because vinyl chloride was involved in the derailment and railcars were burning or being heated. While vinyl chloride is flammable, a significant concern is the generation of toxic combustion products, namely phosgene. On 6 February 2023 a decision was made by the response community to vent the remaining vinyl chloride cars to remove the possibility of a boiling liquid expanding vapor explosion (BLEVE). At approximately 1530 EST time the remaining cars were controlled detonated.

The ASPECT aircraft under the direction of US EPA CMAD assisted US EPA Region 5 in the collection of air monitoring data to support the East Palestine derailment. Notification to activate ASPECT was made late on 5 February 2023 at which time the aircraft was flown to Pittsburgh, PA. Due to low ceilings and icing conditions, the aircraft was unable to fly on 6 February 2023. Weather conditions were favorable for data collection on 7 February 2023 and the aircraft conducted two flight missions. Spectral data collected downwind of the derailment showed no significant detections with only standard components of combustion noted. Thermal analysis showed several cars with elevated temperatures estimated at more than 60C. Primary targets of this deployment included the derailment, the downwind area, and a drainage tributary south of the derailment site. Data collection passes included spectral signatures from the Fourier Transform Infrared Spectrometer (FTIR) and an infrared multispectral line scanner (IRLS). Data was processed using both automated software and manual examination of spectral files against IR libraries. A visible camera was used to record collocated visible information of the various sites. All data was tagged with GPS information to adjust for the correct position on the ground.

Overall, Mission and Collection Design

To support the East Palestine derailment mission, the ASPECT system was employed to collect airborne remote sensed data at a design altitude of 2800 ft above ground level with a ground velocity of 105 kts. By using a programmed lines data collection, passes were made downwind of the derailment in addition to passes over specific target locations as requested by Region-5. On each pass, chemical data was collected using a high-speed (FTIR, a wide area IRLS imaging system, and a set of visible still and video cameras. A detailed description of the ASPECT system can be found in Appendix B. As data was collected, a series of onboard analytical processing routines were used to pre-process all collected data with the results available to a scientific reach-back team on the ground for quality assurance review and overall analysis. Extraction of data from the aircraft was accomplished using a satellite-based communication system.

Upon landing, all raw and pre-processed data was uploaded to a central FTP site for subsequent analysis and quality control (QC) by the scientific reach-back team. Final data products, once reviewed and approved by the Contracting Officer Representative (COR), were uploaded to the Region-5 FTP site.

Data Results

For each data collection pass, the ASPECT system employed three primary sensors concurrently; a Fourier Transform Infrared Spectrometer, (FTIR), an Infrared Line Scanner (IRLS) and a set of visible camera systems to provide visible aerial imagery. The identities and approximate concentrations of target compounds were assessed using both an automated pattern recognition algorithm and by hand analysis of the spectral data.

Using the IRLS sensor, a geo-rectified infrared image was automatically generated for each collection pass. The IRLS uses a similar pattern recognition methodology to that which is used by the FTIR for detection of compounds having spectral characteristics like the common alcohols (ethanol/methanol), ammonia, and isobutylene/butadiene. The result of this product shows the presence of these detections on top of the IR image. It should be noted that while the sensor shows the presence of a compound, the IRLS does not differentiate between specific compounds. In addition, this project feature is not currently part of the automated chemical agent library and was manually processed after the data was transferred from the aircraft.

The still-frame digital mapping camera and a video camera are both bore sighted and slaved to the other detection sensors synchronizing the collection of the chemical information. In general, a visible image is collected every 6 seconds while simultaneously the chemical collection is active with a designed overlap of 30 percent. Each image is orthorectified during processing.

7 February 2023 Results – Flight 1

On 7 February 2023 the ASPECT aircraft conducted a morning flight with the primary mission to document the derailment location and to collect downwind air monitoring data. A secondary collection target included a reconnaissance of the Little Beaver Creek flowing to the south of East Palestine. The aircraft was airborne at 0730 (local) and executed eight (8) data collection passes including two system tests. Figure 1 shows the flight map over the target area. Due to a technical issue with the aerial camera, the recon of Little Beaver Creek was postponed until a later flight.

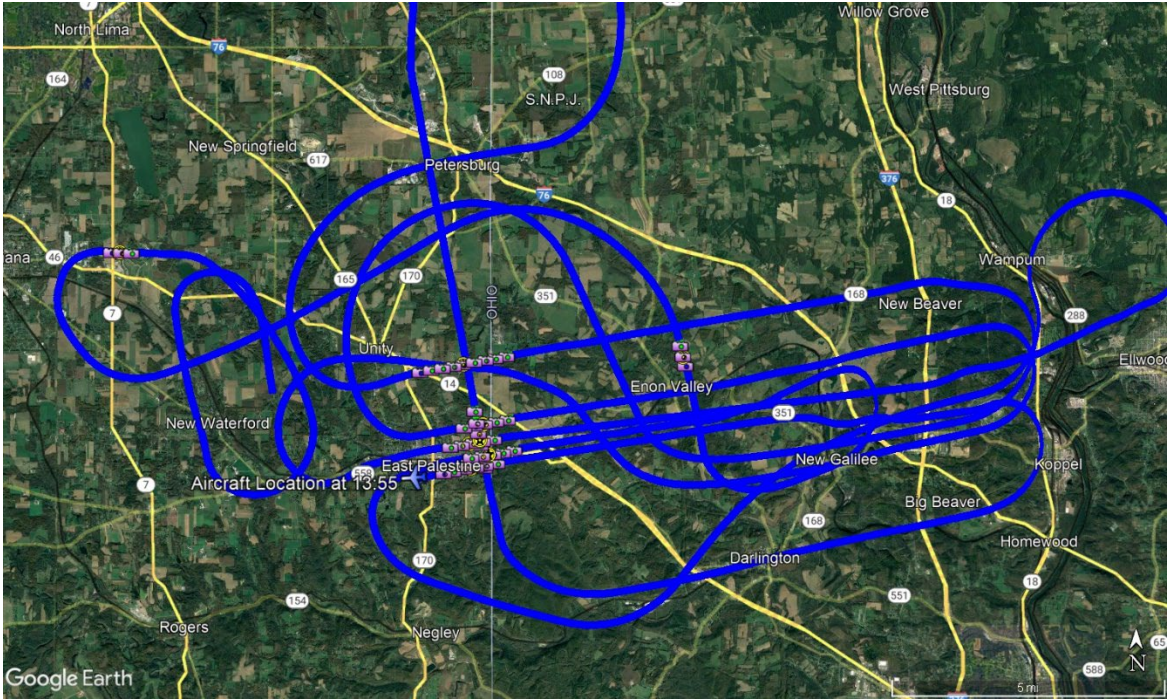


Figure 1. ASPECT Flight Path for 7 February 2023, Flight 1

The weather for the mission was favorable with southerly winds at the surface and moderate winds from the southwest at flight altitude. Turbulence was light to moderate. A summary of mission weather is given in Table 1.

Table 1. Weather Data for Flight 1, 7 February 2023

| Time | 655 | 755 | 855 | 955 | 1055 | 1155 |
|-------------------|-------------------|-------------------|--------------------|-------------------|-------------------|--------------------|
| Wind direction | 180 degrees S | 180 degrees S | 180 degrees S | 202.5 degrees SSW | 202.5 degrees SSW | 225 degrees SW |
| Wind speed | 4.0 m/s (9.0 mph) | 4.0 m/s (9.0 mph) | 4.5 m/s (10.0 mph) | 4.0 m/s (9.0 mph) | 4.0 m/s (9.0 mph) | 5.8 m/s (13.0 mph) |
| Temperature | -1.1 C | -0.6 C | 1.1 C | 2.8 C | 6.7 C | 10.6 C |
| Relative humidity | 83 | 80 | 74 | 67 | 51 | 39 |
| Dew point | -3.3 C | -3.3 C | -3.3 C | -2.8 C | -3.3 C | -2.8 C |
| Pressure | 975.3 mb | 975.0 mb | 975.0 mb | 973.9 mb | 973.6 mb | 972.9 mb |
| Ceiling | Clear | Clear | Clear | Clear | Scattered 4700 Ft | Scattered 4000 Ft |

Automated chemical detection did not identify any compounds within the airborne library. Hand analysis of FTIR data showed low levels of Peroxyacetyl nitrate (PAN), characteristic of combustion. Figure 2 shows a representative spectrum PAN collected immediately downwind of the derailment area. Based on the noise levels of the spectrum, the estimated concentration is less than 1 ppm.

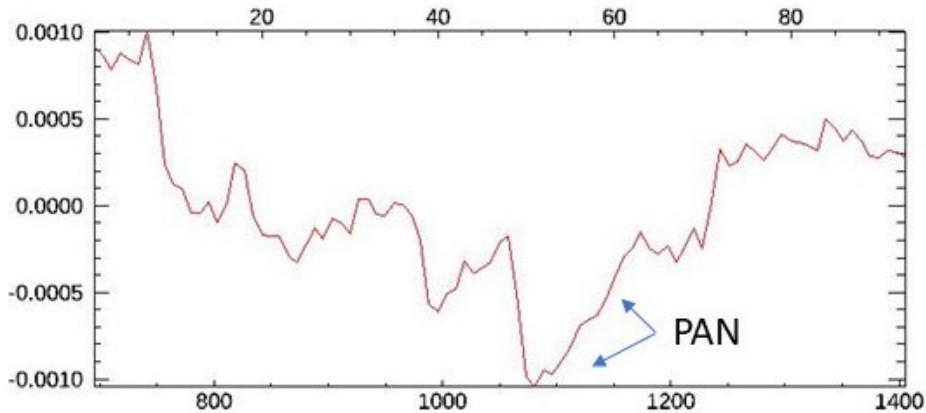


Figure 2. Peroxyacetyl Nitrate Spectrum

Figure 3 shows a three-color image of the derailment area collected with the infrared multispectral lines scanner. The grainy nature of the image is a result of the low thermal contrast over most of the image. Elevated temperatures of derailed cars are evident as white. No plumes are visible in this version of processing. Figure 4 shows a thermal contrast image. The elevated temperatures of the various cars are clear in the image. Figures 5 and 6 show the same image with the temperature ranges shown in color. In the image white is greater than 60C, Red is greater than 22C, Gray is greater than 11C and yellow is the baseline.

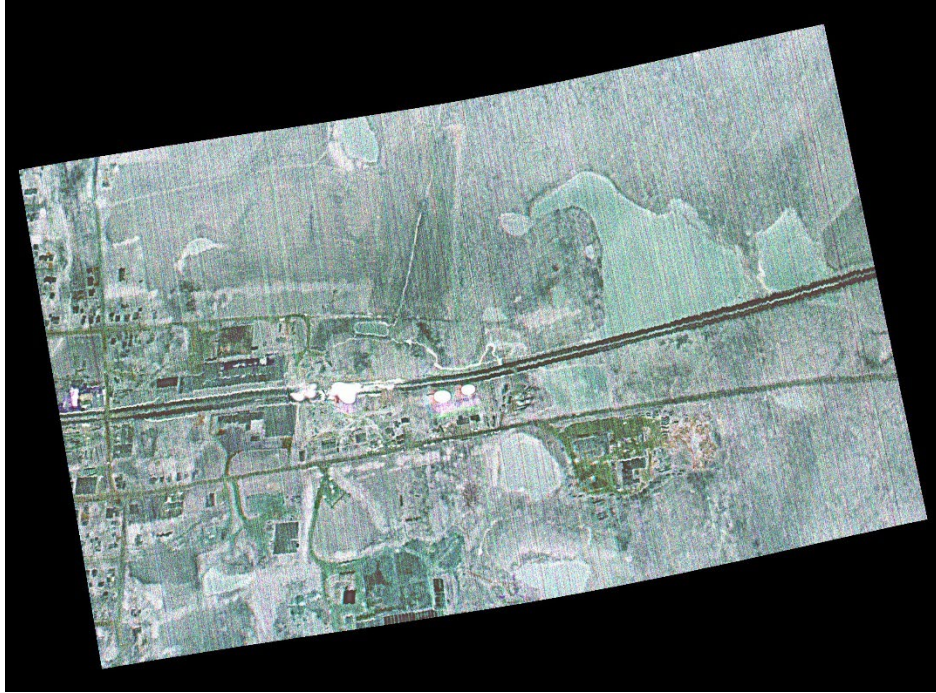


Figure 3. Flight 1, Run 3 Derailment Area.



Figure 4. Flight 1, Run 3 Thermal Contrast Image



Figure 5 Flight 1, Run 3 Thermal Contours.

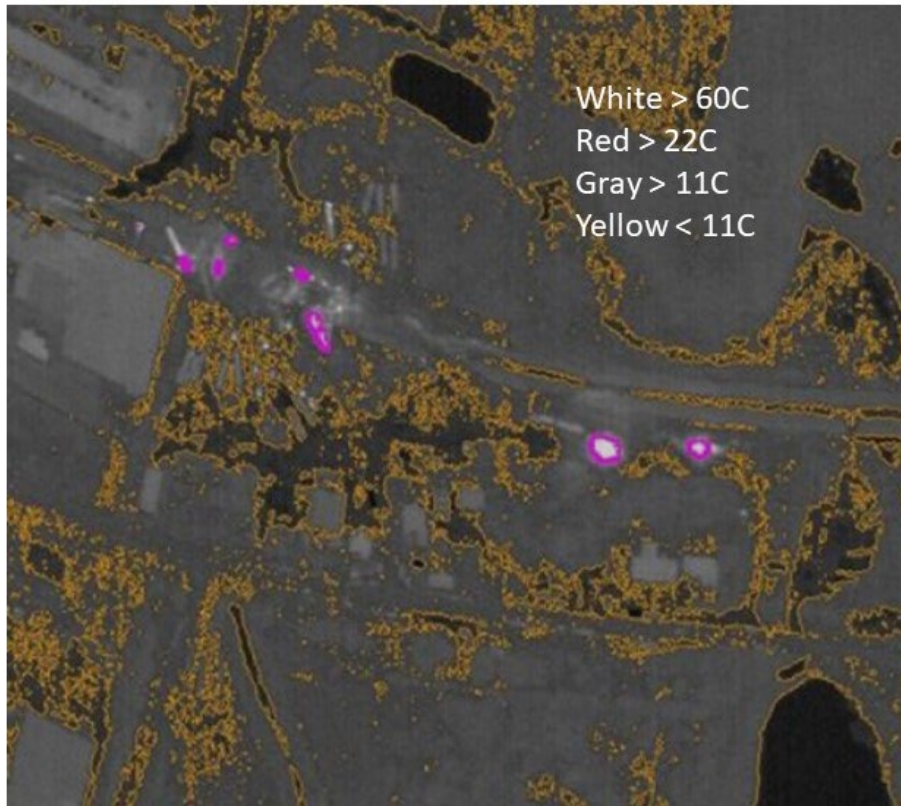


Figure 6. Expanded thermal Analysis Flight 1, Run 3

7 February 2023 Flight 2 Results

A second ASPECT mission was conducted on 7 February 2023 after the issue with the aerial camera was resolved. The primary target area for this flight was Little Beaver Creek in addition to the derailment area. Figure 7 shows the flight path taken to collect additional data over the derailment area while Figure 8 shows the path taken to recon the creek. Between the two locations a total of six (6) data collections were made including two system tests.

Weather for flight 2 was favorable with higher winds and associated turbulence reported at the flight altitude. Surface winds were steady from the south-southwest at moderate velocities. While precipitation was reported in the area, none was reported by the flight crew during the mission.

Table 2. Flight 2, 7 February 2023

| Time | 1155 | 1255 | 1355 | 1455 | 1555 | 1655 |
|-------------------|--------------------|--------------------|--------------------|--------------------|-------------------|--------------------|
| Wind direction | 225 degrees SW | 270 degrees W | 247.5 degrees WSW | 247.5 degrees WSW | 270 degrees W | 292.5 degrees WNW |
| Wind speed | 5.8 m/s (13.0 mph) | 6.3 m/s (14.0 mph) | 6.7 m/s (15.0 mph) | 6.7 m/s (15.0 mph) | 4.0 m/s (9.0 mph) | 4.5 m/s (10.0 mph) |
| Temperature | 10.6 C | 11.1 C | 11.7 C | 12.8 C | 13.3 C | 12.8 C |
| Relative humidity | 39 | 42 | 43 | 45 | 46 | 50 |
| Dew point | -2.8 C | -1.7 C | -0.6 C | 1.1 C | 1.7 C | 2.2 C |
| Pressure | 972.9 mb | 972.6 mb | 971.2 mb | 970.6 mb | 970.9 mb | 972.6 mb |
| Ceiling | Scattered 4000 Ft | Broken 3400 Ft | Scattered 5000 Ft | Scattered 12000 Ft | Overcast 10000 Ft | Overcast 4000 Ft |

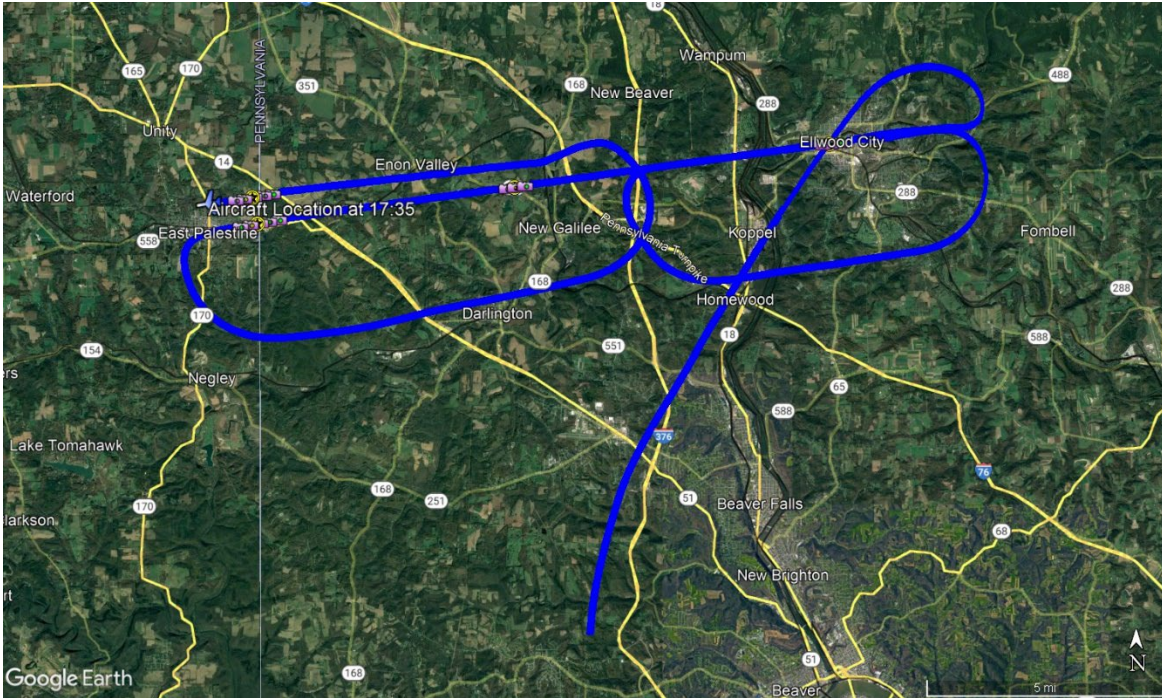


Figure 7 – Flight 2, 7 February 2023 Derailment Area

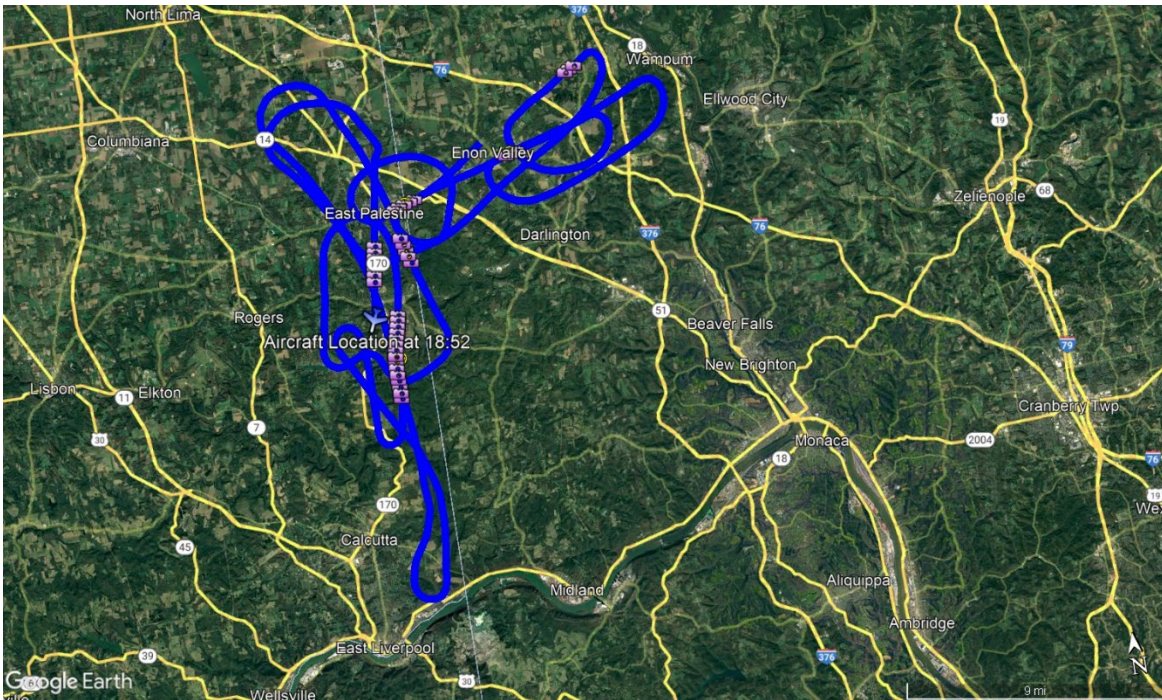


Figure 8. Flight 2, 7 February 2023 Little Beaver Creek

Manual analysis of FTIR data showed no detections from the derailment area other than PAN and ozone. Chemical processing with the IRLS is shown in Figure 9. This processing, while not selective, does indicate a compound within the mid-portion of the

longwave region as evident by the red colored pixels. Cross-analysis with the FTIR indicated that this compound is ozone.

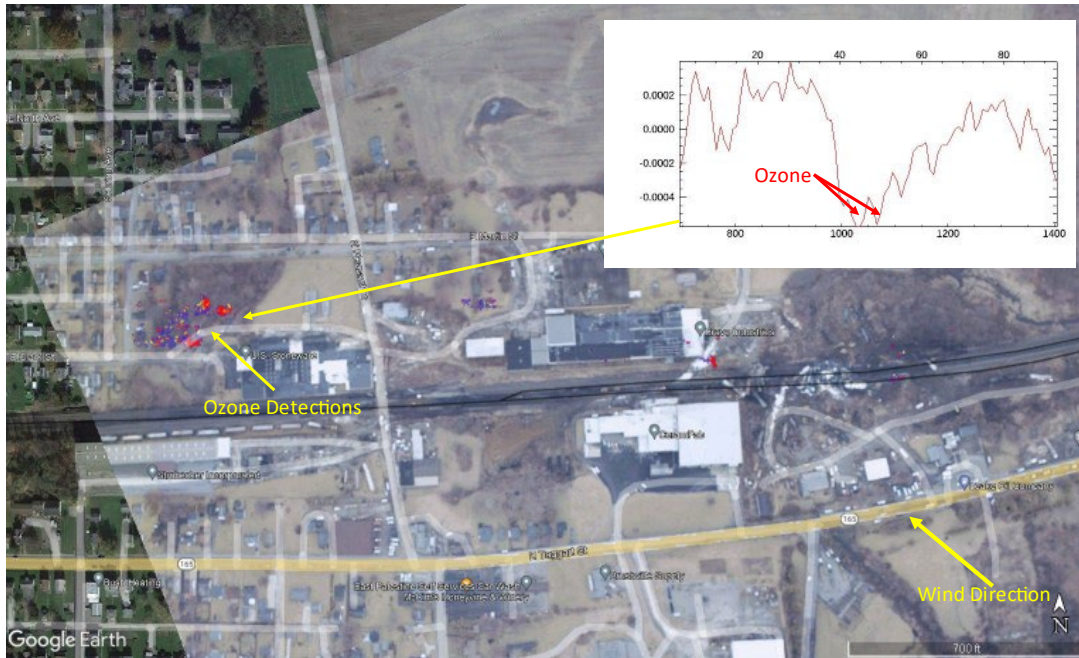


Figure 9. Flight 2, Ozone Detection

Figure 10 shows a representative aerial (oblique) image of the derailment area with a small amount of smoke being emitted from the railcar pile. The location of the pileup and the resulting direction that the smoke is moving shows agreement with the ozone detections seen in Figure 8.



Figure 10. Flight 2, Aerial Image of the Derailment

Conclusion

Data collection in support of the East Palestine derailment showed low detections of PAN and ozone immediately downwind of the derailment. These results indicate that the controlled burn of the railcars was successful. The IRLS imager data processed for thermal contrast indicated that the railcars still showed elevated temperatures over 60C but much less than signatures that would result from a fire.

Table 3. Flight 1 Collection Summary

| Run# | Time (UTC) | Altitude (MSL) | Velocity (knots) | MSIC Data Files | FTIR Data Files | IRLS Data Files | Gamma Files |
|------|------------|----------------|------------------|-------------------------------------------------------------------------------------------------------------------------------------------------------------------------------------------------------------------------------|------------------------------------------------|----------------------------------------------------|-------------|
| 1 | 12:39:52 | 3796 | 89 | 20230207123957804.jpg 20230207124004158.jpg 20230207124010512.jpg | 20230207_123955_A.igm | 2023_02_07_12_39_57_R_01 TA=-3.0;TB=16.1;Gain=3 | |
| 2 | 12:46:16 | 3805 | 98 | 20230207124621822.jpg 20230207124628179.jpg 20230207124633623.jpg | 20230207_124620_A.igm | 2023_02_07_12_46_21_R_02 TA=-5.6;TB=4.7;Gain=3 | |
| 3 | 12:52:38 | 3841 | 100 | 20230207125244026.jpg 20230207125250379.jpg 20230207125255839.jpg 20230207125302180.jpg 20230207125308535.jpg | 20230207_125241_A.igm | 2023_02_07_12_52_43_R_03 TA=-7.0;TB=2.5;Gain=3 | |
| 4 | 13:07:29 | 3847 | 103 | 20230207130735530.jpg 20230207130741886.jpg 20230207130747331.jpg 20230207130753685.jpg 20230207130800041.jpg | 20230207_130734_A.igm | 2023_02_07_13_07_35_R_04 TA=-7.0;TB=3.7;Gain=3 | |
| 5 | 13:19:56 | 3869 | 102 | 20230207132001777.jpg 20230207132008133.jpg 20230207132014486.jpg 20230207132019932.jpg 20230207132026287.jpg | 20230207_131959_A.igm | 2023_02_07_13_20_02_R_05 TA=-6.6;TB=4.1;Gain=3 | |
| 6 | 13:32:31 | 3901 | 101 | 20230207133237106.jpg 20230207133243459.jpg 20230207133248905.jpg 20230207133255260.jpg 20230207133301614.jpg 20230207133307062.jpg 20230207133313416.jpg 20230207133319771.jpg 20230207133326127.jpg | 20230207_133235_A.igm 20230207_133314_A.igm | 2023_02_07_13_32_37_R_06 TA=-6.6;TB=5.5;Gain=3 | |
| 7 | 13:44:17 | 3826 | 108 | 20230207134422501.jpg 20230207134428854.jpg 20230207134434303.jpg 20230207134440655.jpg 20230207134447009.jpg 20230207134452456.jpg | 20230207_134420_A.igm | 2023_02_07_13_44_22_R_07 TA=-6.6;TB=6.2;Gain=3 | |

| | | | | | | | |
|---|----------|------|-----|----------------------------------------------------------------------------------------------------------------------------------------------------|-----------------------|---------------------------------------------------|--|
| 8 | 13:54:14 | 3803 | 103 | 20230207135419861.jpg 20230207135426220.jpg 20230207135431664.jpg 20230207135438020.jpg 20230207135444372.jpg 20230207135449820.jpg | 20230207_135417_A.igm | 2023_02_07_13_54_20_R_08 TA=-6.5;TB=6.0;Gain=3 | |
|---|----------|------|-----|----------------------------------------------------------------------------------------------------------------------------------------------------|-----------------------|---------------------------------------------------|--|

Figure 4. Flight 2 Derailment Area

| Run# | Time (UTC) | Altitude (MSL) | Velocity (knots) | MSIC Data Files | FTIR Data Files | IRLS Data Files | Gamma Files |
|------|------------|----------------|------------------|---------------------------------------------------------------------------------------------------------------------------|-----------------------|---------------------------------------------------|-------------|
| 1 | 17:13:08 | 3824 | 96 | 20230207171314731.jpg 20230207171321086.jpg 20230207171326531.jpg | 20230207_171312_A.igm | 2023_02_07_17_13_14_R_01 TA=6.5;TB=26.5;Gain=3 | |
| 2 | 17:23:40 | 3816 | 103 | 20230207172346592.jpg 20230207172352946.jpg 20230207172358393.jpg | 20230207_172344_A.igm | 2023_02_07_17_23_46_R_02 TA=0.3;TB=20.4;Gain=3 | |
| 3 | 17:26:19 | 3791 | 103 | 20230207172625453.jpg 20230207172631808.jpg 20230207172637264.jpg 20230207172643609.jpg 20230207172649970.jpg | 20230207_172623_A.igm | 2023_02_07_17_26_24_R_03 TA=0.6;TB=20.7;Gain=3 | |
| 4 | 17:35:02 | 3886 | 103 | 20230207173509285.jpg 20230207173514738.jpg 20230207173521094.jpg 20230207173527434.jpg 20230207173532894.jpg | 20230207_173506_A.igm | 2023_02_07_17_35_08_R_04 TA=0.8;TB=20.7;Gain=3 | |

Table 5. Flight 2 Little Beaver Creek Collection Summary

| Run# | Time (UTC) | Altitude (MSL) | Velocity (knots) | MSIC Data Files | FTIR Data Files | IRLS Data Files | Gamma Files |
|------|------------|----------------|------------------|-------------------------------------------------------------------------------------------------------------------------------------------------------------------------------------------------------------------------------------------------------------------------------------------------------------------------------------------------------------------------------------|-----------------|----------------------------------------------------|-------------|
| 1 | 17:58:24 | 3840 | 102 | 20230207175830081.jpg 20230207175836449.jpg 20230207175841886.jpg | | 2023_02_07_17_58_30_R_01 TA=7.7;TB=27.8;Gain=3 | |
| 2 | 18:03:27 | 3785 | 101 | 20230207180333306.jpg 20230207180339657.jpg 20230207180346025.jpg | | 2023_02_07_18_03_33_R_02 TA=-2.3;TB=16.0;Gain=3 | |
| 3 | 18:11:33 | 3855 | 104 | 20230207181139012.jpg 20230207181144460.jpg 20230207181150815.jpg 20230207181157167.jpg 20230207181202615.jpg | | 2023_02_07_18_11_38_R_03 TA=-3.4;TB=13.4;Gain=3 | |
| 4 | 18:22:12 | 3876 | 116 | 20230207182218133.jpg 20230207182224489.jpg 20230207182230844.jpg 20230207182236289.jpg 20230207182242644.jpg | | 2023_02_07_18_22_18_R_04 TA=-1.5;TB=18.4;Gain=3 | |
| 5 | 18:30:32 | 3830 | 107 | 20230207183038358.jpg 20230207183043791.jpg 20230207183050146.jpg 20230207183056512.jpg 20230207183102867.jpg 20230207183108315.jpg 20230207183114669.jpg 20230207183121024.jpg 20230207183126471.jpg 20230207183132825.jpg 20230207183139180.jpg 20230207183144629.jpg 20230207183150982.jpg 20230207183157330.jpg 20230207183202786.jpg | | 2023_02_07_18_30_37_R_05 TA=0.1;TB=20.4;Gain=3 | |
| 6 | 18:50:41 | 3822 | 105 | 20230207185047598.jpg 20230207185053949.jpg 20230207185059395.jpg 20230207185105761.jpg 20230207185112105.jpg 20230207185117552.jpg 20230207185123918.jpg | | 2023_02_07_18_50_46_R_06 TA=0.3;TB=20.3;Gain=3 | |

Appendix A - Table 1. ASPECT Automated Compounds

This table contains ASPECT's library of automated compounds. Detection limits are for each chemical is found in parenthesis in units of parts per million (ppm).

| | | | |
|-----------------------------|-------------------------------|----------------------------|------------------------------|
| Acetic Acid (2.0) | Cumene (23.1) | Isoprene (6.5) | Phosphine (8.3) |
| Acetone (5.6) | Diborane (5.0) | Isopropanol (8.5) | Phosphorus Oxychloride (2.0) |
| Acrolein (8.8) | 1,1-Dichloroethene (3.7) | Isopropyl Acetate (0.7) | Propyl Acetate (0.7) |
| Acrylonitrile (12.5) | Dichloromethane (6.0) | MAPP (3.7) | Propylene (3.7) |
| Acrylic Acid (3.3) | Dichlorodifluoromethane (0.7) | Methyl Acetate (1.0) | Propylene Oxide (6.8) |
| Allyl Alcohol (5.3) | 1,1-Difluoroethane (0.8) | Methyl Acrylate (1.0) | Silicon Tetrafluoride (0.2) |
| Ammonia (2.0) | Difluoromethane (0.8) | Methyl Ethyl Ketone (7.5) | Sulfur Dioxide (15) |
| Arsine (18.7) | Ethanol (6.3) | Methanol (5.4) | Sulfur Hexafluoride (0.07) |
| Bis-Chloroethyl Ether (1.7) | Ethyl Acetate (0.8) | Methylbromide (60) | Sulfur Mustard (6.0) |
| Boron Tribromide (0.2) | Ethyl Acrylate (0.8) | Methylene Chloride (1.1) | Sulfuryl Fluoride (1.5) |
| Boron Trifluoride (5.6) | Ethyl Formate (1.0) | Methyl Methacrylate (3.0) | Tetrachloroethylene (10) |
| 1,3-Butadiene (5.0) | Ethylene (5.0) | MTEB (3.8) | 1,1,1-Trichloroethane (1.9) |
| 1-Butene (12.0) | Formic Acid (5.0) | Naphthalene (3.8) | Trichloroethylene (2.7) |
| 2-Butene (18.8) | Freon 134a (0.8) | n-Butyl Acetate (3.8) | Trichloromethane (0.7) |
| Carbon Tetrachloride (0.2) | GA (Tabun) (0.7) | n-Butyl Alcohol (7.9) | Triethylamine (6.2) |
| Carbonyl Fluoride (0.8) | GB (Sarin) (0.5) | Nitric Acid (5.0) | Triethylphosphate (0.3) |
| Carbon Tetrafluoride (0.1) | Germane (1.5) | Nitrogen Mustard (2.5) | Trimethylamine (9.3) |
| Chlorodifluoromethane (0.6) | Hexafluoroacetone (0.4) | Nitrogen Trifluoride (0.7) | Trimethyl Phosphite (0.4) |
| Chloromethane (12) | Isobutylene (15) | Phosgene (0.5) | Vinyl Acetate (0.6) |

Appendix B. ASPECT Sensor System Description

The ASPECT sensor suite (Figure 1) is mounted in a fixed wing aircraft and uses the principles of remote hazard detection to image, map, identify, and quantify chemical vapors and deposited radioisotopes. Chemical plume measurements are made at a rate of about two square miles per minute. The system normally operates at an altitude of 2800 feet above ground level (AGL) and results in a high IR spatial resolution of 0.3 meters. A simplified system diagram is provided in Figure 2. The radiological data is collected between 300 and 500 feet AGL with a collection time of once per second and a field of view about 600-1000 feet. Situational awareness is provided by using both high-resolution aerial digital photography and digital video that are concurrently collected with chemical and radiological data and forms the basis for a geographical information system data cube with several layered data products (Figure 3). Efficient mission execution requires that data is processed on-board the aircraft for transmission or hand-off to the first responder. To facilitate data transmission while in flight status, the aircraft is equipped with a broadband high-speed satellite data communications system. With a combination of onboard data processing and the satellite communication system, selected airborne situational data sets are ready for dissemination to the incident command team in less than 5 minutes after collection.

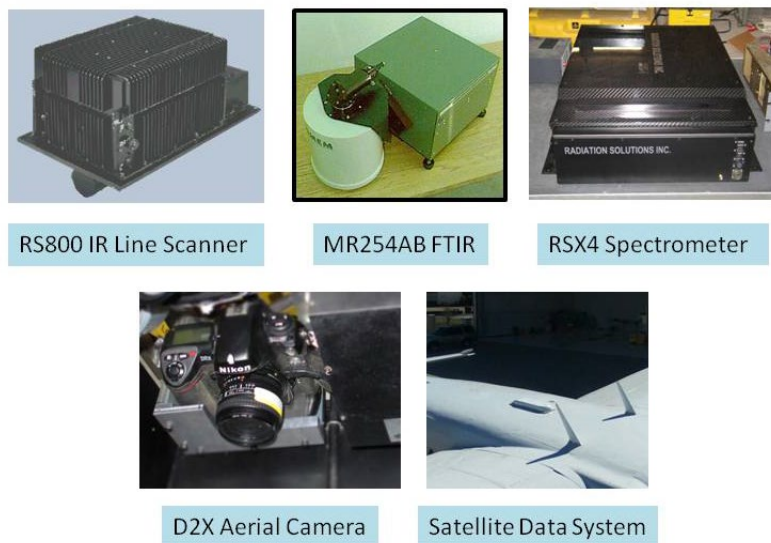


FIGURE 1 – Sensor Suite

NOTE: Images of the neutron detector and LaBr detectors are not shown. The aircraft is equipped with three RSX-4 units, only one is shown in this figure.

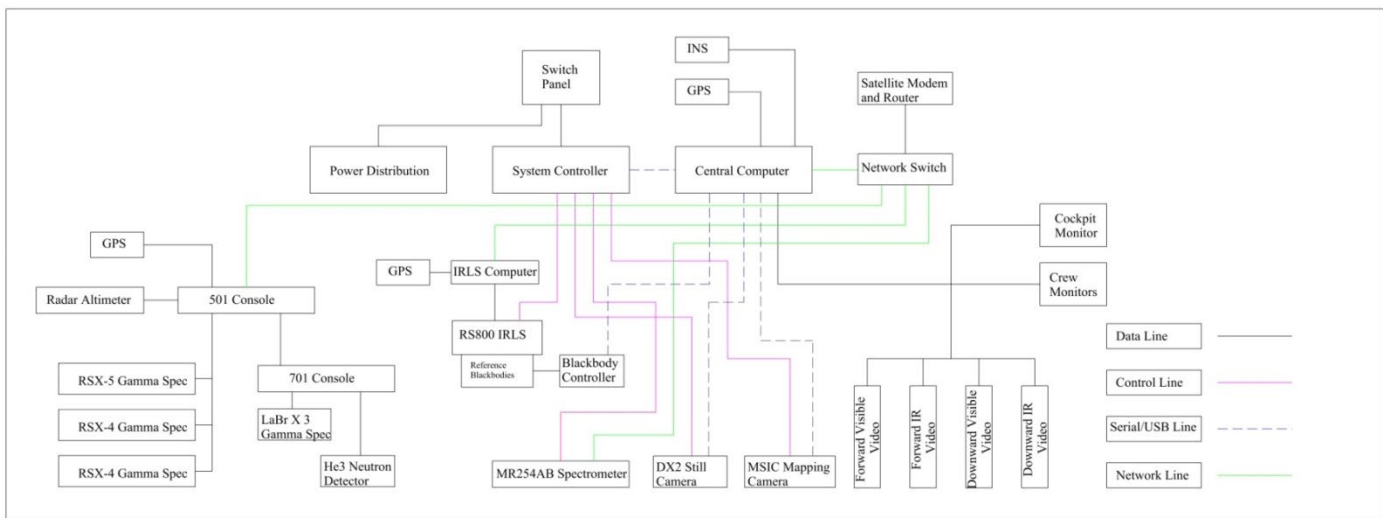


FIGURE 2 - Simplified ASPECT System Diagram

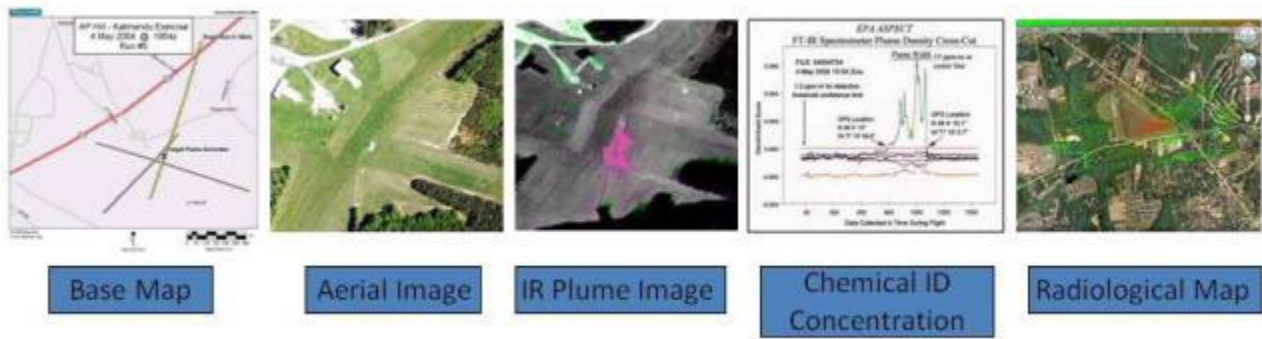


FIGURE 3 – Data Products

1. Airframe

The ASPECT sensor suite is operated from a single engine Cessna 208B Cargo Master aircraft (Figure 4). The aircraft and crew are certified for full instrument flight rules (IFR) flight operations. This aircraft is equipped with one 20 X 30-inch belly hole with a retractable bay door. All sensor systems are mounted on vibration isolated base plates positioned over the belly hole. The aircraft can operate from any airport having a 3000 ft runway and can stay aloft for 5 hours. Technical specifications for the program airframe are contained in Table 1.



FIGURE 4 – ASPECT Aircraft, N9738B

TABLE 1 – N9738B Technical Specifications

| | |
|-----------------------|---------------------------------------------------------------------------------------|
| Tail: | N7938B |
| System: | Single Engine Turbo-Propeller Driven Aircraft |
| Make: | Cessna 208B Cargo Master, Part 91 Certification |
| Power Plants: | Pratt and Whitney PT-6A-114 turbine driven three blade propeller, 600 shaft HP |
| Empty Weight: | 4458 lbs. |
| Useful Weight: | 4604 lbs. |

| | |
|---------------------------------|--------------------------------------------------------------------------------------------------------------------------------------------------------------------------------------------------------------------------------------------------------------|
| Maximum Take-off Weight: | 9062 lbs. |
| Typical Cruise Speed: | 160 Kts |
| Typical Flight Duration: | 6 Hours (65% Power) Plus 45 Minute Reserve |
| Service and Ceiling: | Low Altitude Waiver, 25000 Ft (MSL) max altitude |
| Cabin: | Un-pressurized, Crew Oxygen |
| Portals: | One, 20 X 30 inch STC sensor- hole with Remote Door |
| Avionics | GPS IFR Package GPS navigation system for programmed flight lines Terrain/Obstacle Avoidance Equipped Radar Altimeter Equipped Dual weather Radar, Live Weather Feed Dual VOR Equipped, Dual Comms Equipped Dual Transponders |
| Electrical Buss: | Primary, 28 vdc @ 200 amps full load Secondary, 28 vdc @ 90 amps full load |
| Data Communication: | Phased Array Satellite System, 40-60 KB/sec Data/Telephone combined |
| Readiness Status: | 24/7/365 |

2. Chemical Detection Capabilities

The principle of remote detection, identification, and quantification of a chemical vapor species is accomplished using passive infrared spectroscopy. Most vapor compounds have unique absorption spectral bands at specific frequencies in the infrared spectral region. An asymmetric stretching between two atoms in a molecule result in a fundamental frequency of vibration. Passive infrared measurements of a vapor species are possible due to small thermal radiance differences between the temperature of the chemical plume and a particular infrared scene background (Figure 5). Both the cloud and the atmosphere contribute to the total emitted radiance measured by an infrared sensor. Careful monitoring of the change in total infrared radiance levels leads to concentration estimations for a particular vapor species. Concentration times path length estimations are obtained based on the molar absorptivity for each vapor species.

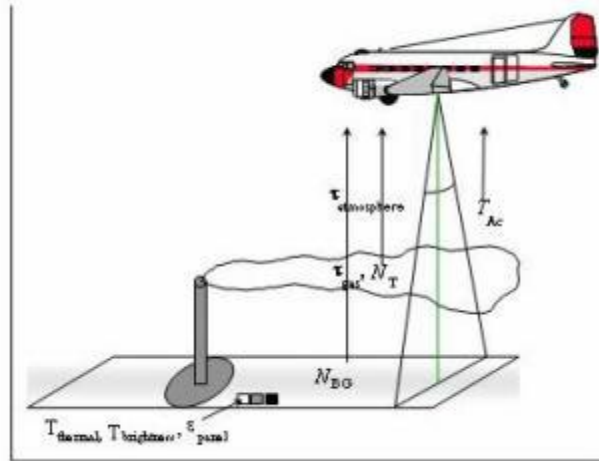


FIGURE 5 - Principles of Remote Infrared Detection

A. RS800IRLS Infrared Imager Sensor

The ASPECT Program uses a modified Raytheon RS800 infrared line scanner to generate wide area chemical imagery (Figure 6). This system incorporates a unique detector assembly consisting of 16 cryogenically cooled optical band pass filters affixed to a focal plan array. Scanning is accomplished with an integrated rotating prism controlled by a feedback motor scan controller. Each rotation of the prism sweeps an angular field of view of 60 degrees resulting in 1500 data points. When the scan rate is coupled to the normal 110-knot ground speed of the aircraft, a scan swath of 0.5 meters is collected. This collection geometry outputs a square data pixel 0.5 X 0.5 meters square. Radiometric calibration is performed during each prism rotation by viewing two reference blackbodies mounted on either side of the unit. Image registration is accomplished during post processing by incorporating pitch and roll data collected from an integrated gyroscope mounted on the scanner body. An integrated GPS receiver is used in the processing step providing geo-registration of each pixel in the finished image product. Detailed specifications of the RS800IRLS are contained in Table 2.



FIGURE 6 - RS800IRLS Line Scanner

TABLE 2 - RS800IRLS Technical Specifications

| | |
|-------------------------------------|------------------------------------------------------------------------------------|
| System: | TI Systems/Raytheon RS800 MSIRLS |
| Detector: | Cryogenically cooled focal plane array with integrated cold optical filters |
| Spectral Coverage: | 3 – 5 micrometer (mid-wave) and 8 – 12 micrometers (long-wave) |
| Number of Spectral Channels: | 16 total, 8 mid-wave and 8 long-wave |
| Spectral Resolution: | 5 to 20 wave numbers, channel dependent |
| Spatial Resolution: | Better than 1.0 mill radian |
| Scan Rate: | 60 Hz |
| Radiometric Calibration: | Two flanking blackbody units |
| Field of View (FOV): | 60 Degrees |
| Thermal Resolution | 0.05 Degree C. |
| Linear Range | 0 to 200 Degree C |
| Pixel Resolution (IFOV): | 0.5 meters @ 850-meter collection altitude (AGL) |
| Cross Field Scan Coverage: | 980 meters @ 850-meter collection altitude (AGL) |
| Attitude Stabilization: | 25 Hz pitch and roll providing stabilized video |
| Power: | 28 vdc @ 10 amps full load |
| Weight: | 27 Kg (60 lbs.) |
| Spin-up Time: | Less than 12 minutes (including cryo-system) |

| | |
|--------------------------|------------------------------------------------------------------------------------------------------------------------|
| Standard Outputs: | 2 Channels of stabilized RS-170 video, 16 channels of digitized (16 bit) spectral data, 1 channel of GPS (2 Hz) |
| Data Processing | 1 step full radiometric image generation using an onboard algorithm. Approximately 1 minute processing time. |

B. IRLS - Chemical Image Processing

1. Chemical Processing

Processing of chemical data is divided into two broad categories including image processing and spectral processing. Infrared chemical signatures present a challenge in data processing due to the small signal to noise ratio (SNR) of the chemical vapor between the sensor and the surface. It is not uncommon to have a SNR of less than four in a typical vapor cloud. In order to image such a weak signal, the collection system and detector must be optimized for high collection efficiency and a small instantaneous field of view. The ASPECT RS800IRLS meets both requirements by using an F/1 high-speed optical train coupled to a 16-channel cold optical filter focal plane array. This configuration provides very high signal throughput while maintaining a 1.0 mill radian spatial resolution. The use of cold optical band pass filters directly mounted on the face of the focal plane array eliminates a large portion of the self-radiance (noise) while minimizing the attenuation of wanted signal content. Raw data is fully radiometrically calibrated using a set of flanking blackbodies providing radiance-adjusted imagery. Jitter removal and band registration are accomplished using an automated algorithm using an integrated 2-dimensional gyro and GPS feed. Final data is generated using an automated geo-registration algorithm in either a geo-Tiff or a geo-Jpeg format. Processing can be accomplished while in flight and requires about 30 seconds to 1 minute per image depending on size. The completed imagery is compressed and made available to ground user through the aircraft satellite link.

The vapor cloud, shown in Figure 7, is captured in an infrared image collected by the RS800SIRLS multispectral sensor at an industrial site in the Midwest. The detection limit of the vapor concentration (shown in red) was determined to be less than 20 ppm/m while the center cloud concentration was greater than 250 ppm/m. This image has been cropped with only 1/3 of the actual sensor field-of-view being displayed. The original image width of the image was approximately 1200 meters wide. For the ASPECT application, the RS800IRLS system provides a qualitative indication of the presence or

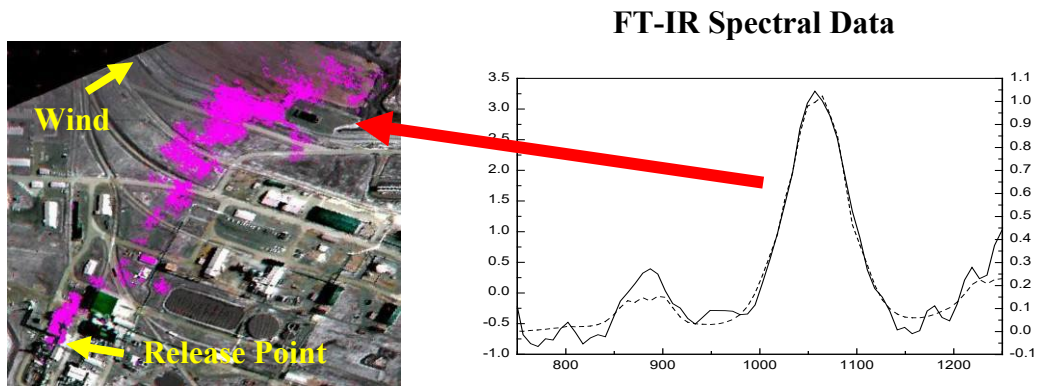


Figure 7 - RS800IRLS Data Product

absence of a particular chemical species. The detection limit provided by the sensors is applicable to both chemical emergency response and crisis mitigation following a terrorism event.

2. Thermal Processing

Figure 8 shows a long wave thermal image of an underground mine fire in Kansas City, MO. In this application, the calibrated radiometric data from the RS800IRLS is processed to show direct surface temperature. In the standard configuration, the imager provides an automated linear temperature measure up to about 200 °C at a resolution of 0.05 °C. Higher temperature measurements in the order of 500 °C are possible by changing the input stop and detector of the instrument. As part of the thermal processing method, solutions to the scene emissivity are solved and factored into the temperature product.

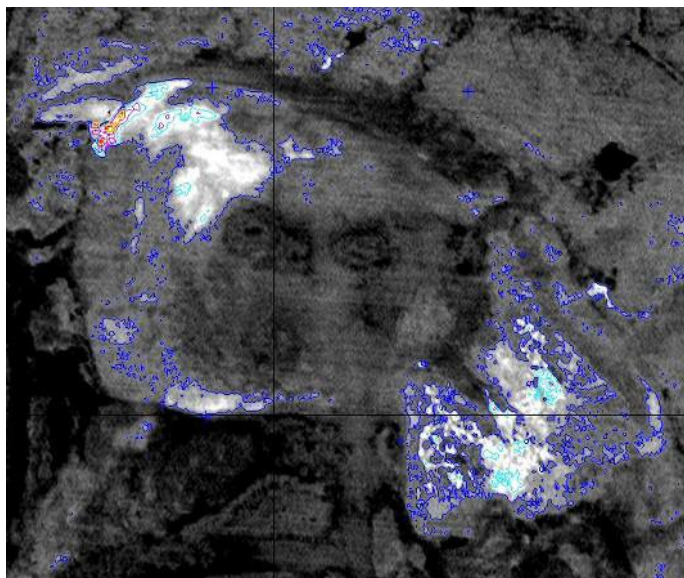


FIGURE 8 - Thermal Image of an Underground Mine Fire

3. Oil Detection Processing

The ASPECT sensor system was extensively used to detect oil on water during the Deep Water Horizon Oil spill. The application of long wave IR to detect oil has been known for several years and has advantages over visible detection of oil including the ability to image oil under strong sun angle (glint) and the ability to image oil at night. The primary problem of using long wave IR in oil detection is centered on an accurate measure of the surface temperature with a pixel size that is small enough to provide adequate scene dynamic range. Figure 9 shows an image that was processed from oil on water in the open ocean. In this setting, the surface temperature of the ocean is very constant. The image was formed by detecting the difference in emissivity between 0.96 for water and 0.93 for oil. Weathered oil has an emissivity of 0.98 or 0.99 and was usually at a different surface temperature. This image was processed using the small emissivity differential of oil and water as the primary discriminate, coupled with weather oil having a different surface temperature.

By using a processing technique that examined data value boundaries, the amount of oil on the water surface was generated. Figure 10 shows an image of oil on water in a near shore environment. For this environment, the thermal gradient of the water in the shallows is much greater than the emissivity contrast of the oil and water. A multi-dimensional pattern recognition algorithm utilizing a pre-processing procedure known as alpha residuals to eliminate the temperature difference was used to discriminate oil and water. This technique permitted detection and characterization of oil ranging from sheen to thick oil.

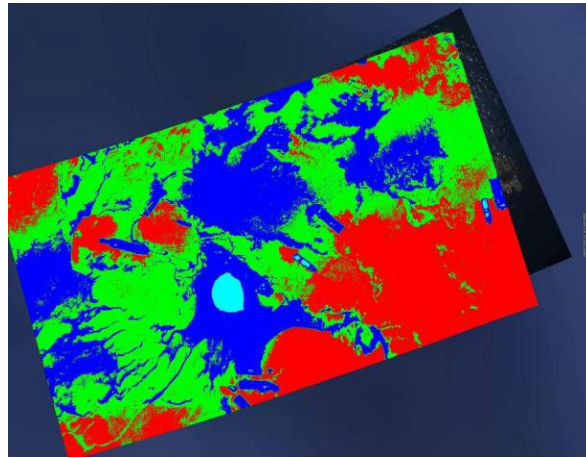


FIGURE 9 - Open Water Detection and Discrimination of Oil Using IR

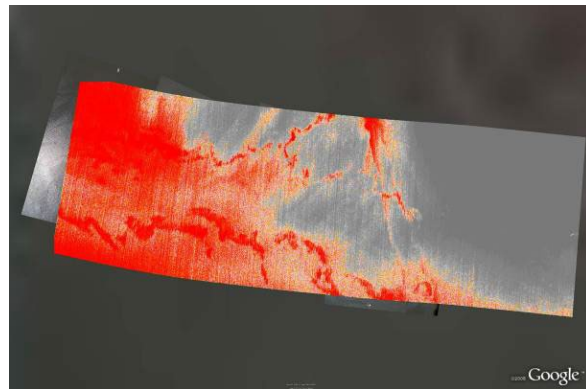


FIGURE 10 - Detection and Discrimination of Oil using Pattern Recognition

C. MR254AB Spectrometer

Chemical vapor detection and quantification is accomplished using a modified Bomem MR254AB spectrometer (Figure 11). This custom designed spectrometer utilizes a double wishbone pendulum interferometer providing both high signal throughput and vibrational noise immunity. Two cryogenically cooled detectors provide both mid and long wave operation. Spectral resolution is selectable and ranges from 1 to 128 wave number with 16-wave number normally used for automated compound detection. When operated at 16 wave number resolution, the unit scans at 70 Hz providing a spatial sampling interval every 0.75 meters along the ground track of the aircraft. The program uses an automated compound detection algorithm based on digital filtering and pattern recognition. Geo-registration of each Fourier Transform Spectrometer (FTS) scan is accomplished using a concurrent GPS input from the ASPECT main GPS receiver. Technical specifications of the FTS system are contained in Table 4.



FIGURE 11 - MR254AB FTS Spectrometer

TABLE 4 - FTS Technical Specifications

| | |
|--------------------|-------------------------------------------------------------------------------------------------|
| System: | Modified Bomem MR-200 Series (MR-254AB) |
| Detectors: | Cryogenically cooled Single Pixel Design |
| Spectral Coverage: | InSb Detector for 3 – 5 micrometer (mid-wave) MCT Detector for 8 – 12 micrometer (long-wave) |

| | |
|------------------------------|----------------------------------------------------------------------------------------------------------------------------------------------------------------|
| Noise Figure | Mid-wave 6×10^{-9} W/cm²-srcm⁻¹, Long-wave 1.8×10^{-8} W/cm²-srcm⁻¹ |
| Spectral Resolution: | 1 to 128 wave numbers, User selectable |
| Spatial Resolution: | 5 milli-radian (0.2°) thru 25.4 cm (10 inch) Primary Telescope, 0.75 meter interval at 110 kts collection velocity |
| Scan Rate: | 70 Hz @ 16 wave number resolution |
| Field of View (FOV): | 3 meters @ 850-meter collection altitude (AGL) |
| Radiometric Reference | Integrated cold source (77° K) |
| Targeting | Calibrated bore camera (Nadir) |
| Power: | 28 vdc @ 8 amps full load |
| Weight: | 40 Kg (90 lbs.) |
| Spin-up Time: | Less than 4 minutes (including cryo-system) |
| Standard Outputs: | 2 Channels of Grams format spectral data (16 bit), 1 channel of RS-170 video. |
| Data Processing: | 1 Step pattern recognition compound detection using onboard algorithms, approx. 30 – 60 seconds processing time after data collection. |

D. Spectral Processing

Spectral data processing (signal processing) from the ASPECT MR-254AB spectrometer is processed using background suppression, pattern recognition algorithm. Processing spectral data from a moving airborne platform requires unique methods to balance weak signal detection sensitivity, false alarm minimization, and processing speed. The background suppression, pattern recognition methods associated with the ASPECT Program have been documented in over 100 open literature publications. One of the principal weaknesses of airborne FTS data is the ability to reference each collected spectra to a suitable background for subsequent spectra subtraction. While methods have been devised to accomplish this procedure, typical airborne spectra show changes between successive scan of several orders of magnitude due to changing radiometric scene conditions. These scan-to-scan changes render traditional background subtraction methods unusable for weak signal detection. The background suppression method used by ASPECT circumvents this problem by using a digital filtering process to remove the background component from the raw interferometer data. This approach is analogous to using the tuning section of a radio receiver to preselect the portion of the signal for subsequent processing. The resulting filtered intermediate data maintains the weak signal components necessary for subsequent analysis.

An additional weakness of traditional FTS processing involves the need to provide a resolution high enough to permit compounds exhibiting narrow spectra features to be matched with published library spectra. This method is initiated using the Fast Fourier Transform (FFT). While the FFT algorithm is very robust mathematically, certain data collection requirements must be met to permit the transform to be valid. To provide high spectral resolution spectra, the length of the interferogram must be matched to the desired resolution for the transform to work properly. This requirement forces a long collection period for each interferogram and since the aircraft is moving, it is probable that the radiometric scene being viewed by the spectrometer will change during the collection of the interferogram. The changing scene causes the FFT to generate spectral artifacts in the resulting spectral information. These artifacts are phantom signals that confuse and complicate subsequent compound identification.

The standard matched filter compound discrimination method likewise exhibits weak signal performance and often generates false alarms due to common atmospheric interference. ASPECT solves these problems by using a combination of digital band pass filtering followed by a multi-dimensional pattern recognition algorithm. The digital filters and pattern recognition coefficients are developed using a combination of laboratory, field, and library data and folded into a training set that is run against unknown data. Digital filters can be readily constructed which consider both spectrometer line shapes and adjacent interferents, greatly improving the weak signal system gain. The pattern recognition algorithm processes the filter output in a multi-space fashion and enhances the selectivity of the detection. These methods are very similar to a superheterodyne receiver that uses band pass adjustable intermediate filters followed by a DSP detector/discriminator such as in a modern radar system. Since the methods use relatively simple computational operations, signal processing can be accomplished in a few seconds. Finally, as data is processed, the position of the detection is referenced to onboard GPS data providing a GIS ready data output. Table 6 lists the compounds (and a 10-meter equivalent path length detection limit) that are currently installed in the airborne library using the digital filtering/pattern recognition method.

A unique feature of the ASPECT System includes the ability to process spectral data automatically in the aircraft with a full reach back link to the program QA/QC program. As data is generated in the aircraft using the pattern recognition software, a support data package is extracted by the reach back team and independently reviewed as a confirmation to data generated by the aircraft. Figure 12 shows airborne absorbance spectra of ammonia vapor collected from an ammonium nitrate fire using the MR-254AB spectrometer. This spectrum was generated by carefully selecting a suitable background spectrum and conducting a traditional background subtraction, a time-consuming operation. Figure 13 shows the same data processed using the automated background suppression/pattern recognition method. Ammonia detection is clearly demonstrated. Figure 14 shows how these detections are referenced to a real-world geographical map. Individual detection locations corresponding to FTS scans are mated with latitude and longitude coordinate values.

TABLE 6 - Chemicals Included in the ASPECT Auto-Processing Library

| | | | |
|-----------------------------|-------------------------------|------------------------------|-----------------------------|
| Acetic Acid (2.0) | Cumene (23.1) | Isoprene (6.5) | Propylene (3.7) |
| Acetone (5.6) | Diborane (5.0) | Isopropanol (8.5) | Propylene Oxide (6.8) |
| Acrolein (8.8) | 1,1-Dichloroethene (3.7) | Isopropyl Acetate (0.7) | Silicon Tetrafluoride (0.2) |
| Acrylonitrile (12.5) | Dichloromethane (6.0) | MAPP (3.7) | Sulfur Dioxide (15) |
| Acrylic Acid (3.3) | Dichlorodifluoromethane (0.7) | Methyl Acetate (1.0) | Sulfur Hexafluoride (0.07) |
| Allyl Alcohol (5.3) | 1,1-Difluoroethane (0.8) | Methyl Ethyl Ketone (7.5) | Sulfur Mustard (6.0) |
| Ammonia (2.0) | Difluoromethane (0.8) | Methanol (5.4) | Nitrogen Mustard (2.5) |
| Arsine (18.7) | Ethanol (6.3) | Methylbromide (60) | Phosgene (0.5) |
| Bis-Chloroethyl Ether (1.7) | Ethyl Acetate (0.8) | Methylene Chloride (1.1) | Phosphine (8.3) |
| Boron Tribromide (0.2) | Ethyl Formate (1.0) | Methyl Methacrylate (3.0) | Tetrachloroethylene (10) |
| Boron Trifluoride (5.6) | Ethylene (5.0) | MTEB (3.8) | 1,1,1-Trichloroethane (1.9) |
| 1,3-Butadiene (5.0) | Formic Acid (5.0) | Naphthalene (3.8) | Trichloroethylene (2.7) |
| 1-Butene (12.0) | Freon 134a (0.8) | n-Butyl Acetate (3.8) | Trichloromethane (0.7) |
| 2-Butene (18.8) | GA (Tabun) (0.7) | n-Butyl Alcohol (7.9) | Triethylamine (6.2) |
| Carbon Tetrachloride (0.2) | GB (Sarin) (0.5) | Nitric Acid (5.0) | Triethylphosphate (0.3) |
| Carbonyl Chloride (0.8) | Germane (1.5) | Nitrogen Trifluoride (0.7) | Trimethylamine (9.3) |
| Carbon Tetrafluoride (0.1) | Hexafluoroacetone (0.4) | Phosphorus Oxychloride (2.0) | Trimethyl Phosphite (0.4) |
| Chlorodifluoromethane (0.6) | Isobutylene (15) | Propyl Acetate (0.7) | Vinyl Acetate (0.6) |

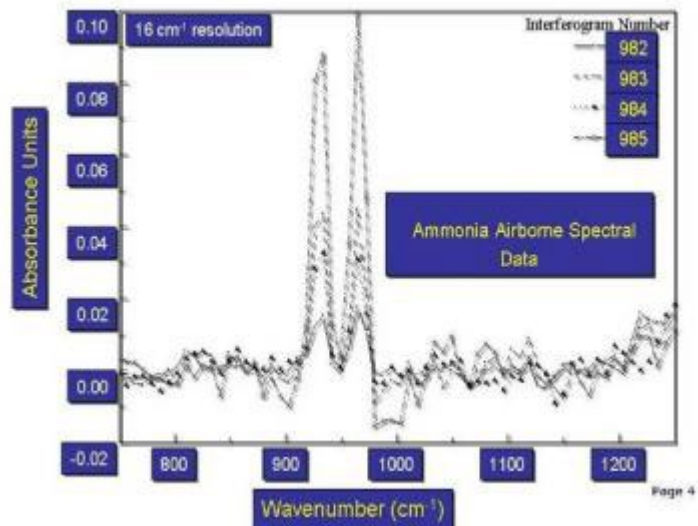


FIGURE 12 - Ammonia Spectra

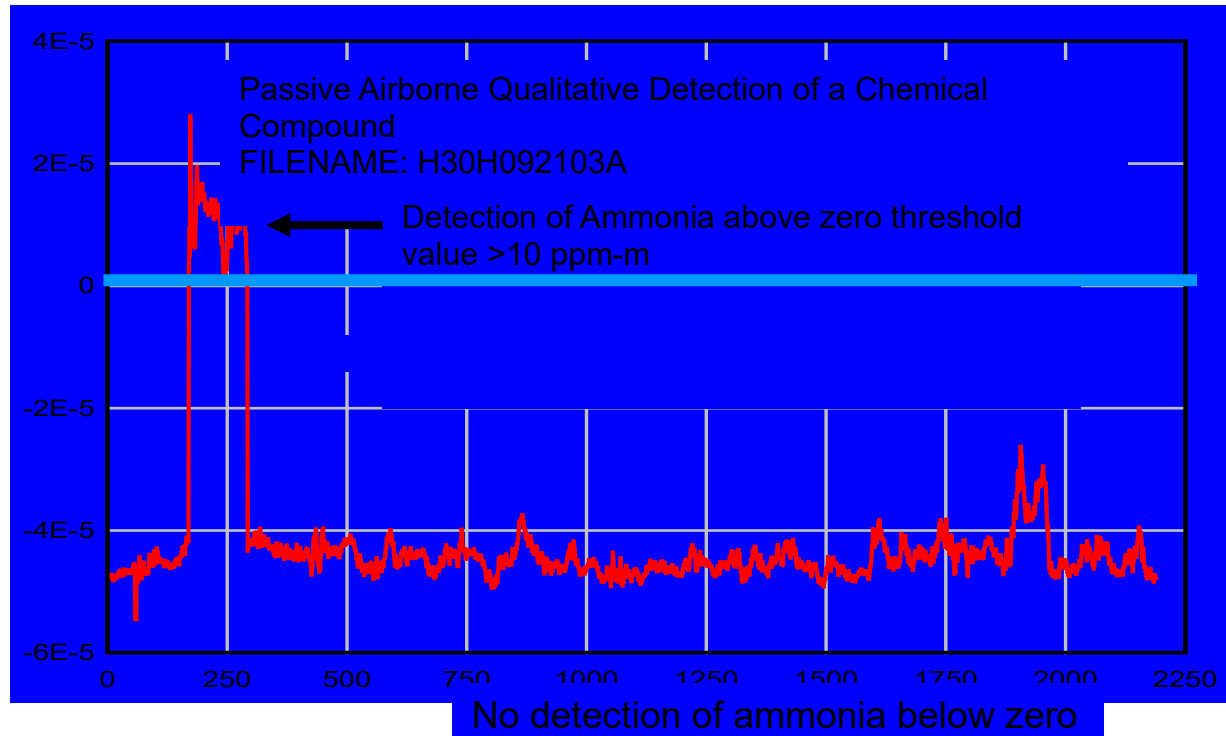


FIGURE 13 - Ammonia Detected with Pattern Recognition



FIGURE 14 - Locations of Ammonia Detection

Quantitative compound specific information is also generated using the MR-254AB spectrometer. This application uses a multi-dimensional model generated using radiometric, thermal, and concentration calibrated laboratory data for each compound in the airborne library. As with compound detection methods, multiple publications have documented the feasibility of using this approach to remotely quantify chemical vapors. The first open literature scientific peer reviewed paper was completed using the ASPECT method.

Figure 15 shows the estimated concentration of methanol measured by ground sensors and compared with the remotely collected FTIR data. The data shows a standard error of prediction of 18 ppm-m for a range of concentration between 20 to 400 ppm-m. This range of concentrations is consistent with both hazardous vapor releases and terrorist concerns.

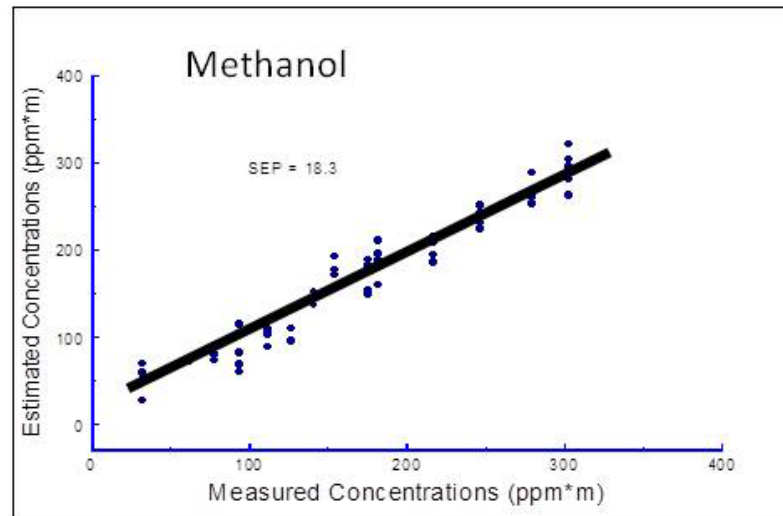


Figure 15 - Quantitative Methanol Results

3. Radiological Detection Capabilities

A. RSX4 Sodium NaI Gamma Ray Spectrometers

Airborne radiological measurements are conducted using three fully integrated multi-crystal sodium iodide (NaI) RSX4 gamma ray spectrometers (Figure 16). Each RSX4 spectrometer contains four 4"x2"x16" doped NaI crystals each having an independent photomultiplier/ spectrometer assembly. One RSX unit is configured with an additional upward NaI crystal utilized to provide real-time cosmic ray correction. Count and energy data from each crystal and pack is combined using a self-calibrating signal processor to generate a virtual detector output. All spectrometer "packs" are further combined using a signal console controlled by the on-board computer in the aircraft. Due to the advanced signal processing techniques unique to the RSX4 units, very high total count rates (approximately 1 million counts per second) can be discriminated and processed. Specifications of the RSX4 spectrometers can be found in table 8.

B. Lanthanum Bromide Gamma Ray Spectrometers

High resolution gamma ray detection is provided using a set of three 3" x 3" lanthanum bromide (LaBr) crystals all ganged into a single virtual detector. This configuration of detector has a much lower efficiency but has a much higher degree of spectral resolution than the NaI spectrometers. Accordingly, the LaBr crystal are most often used in complex isotope environments having a higher intensity such as in a fall-out field resulting from a nuclear accident.

Neutron detection is provided using a set of two, four bundle straw neutron detectors. These systems do not use expensive and rare He3 gas and are very rugged. Both detectors are ganged into one virtual total count sensor. Radiological spectral data, GPS position, and radar altitude are always collected at a one-second intervals during a survey. In order to provide optimal collection geometry, flight line data is loaded into the aircraft flight computer prior to conducting the survey. Typical airborne surveys are flown at 300 to 500 feet AGL.



FIGURE 16 - RSX4 Gamma Ray Spectrometer

C. Neutron Detection

Proper spectrometer operation and data quality assurance is maintained using both internal and external calibration algorithms. A self-contained internal calibration algorithm acts as a watchdog and continuously monitors the spectrometer systems for proper system operation and data output. If any errors are encountered with a specific crystal and/or spectrometer pack during the collection process an error message is generated, and the data associated with that crystal are removed from further analyses. External calibration procedures are routinely executed and consist of both designed data collection over characterized areas and pad calibrations over

known quantities of radiological doped concrete. Technical specifications for the RsX4 gamma ray spectrometers are contained in Table 8.

TABLE 8 - RX4 Technical Specifications

| System: | RSI RSX4 Gamma Ray Spectrometer |
|-----------------------------------|---------------------------------------------------------------------------------------------------------------------------------------|
| Detector: Gamma Ray | 4 Doped NaI Detectors per pack, 3 Packs, 2x4x16 inch crystals, |
| Detector: Cosmic Ray | One 2x4x16 upward crystal integrated into one of the RSX units. |
| Total NaI Detector Volume: | 25 liters |
| Energy Coverage: | 0 – 3000 KeV |
| Number of Channels: | 1024 |
| Energy Resolution: | Approx. 3 KeV per Channel |
| Scan Rate: | 1 Hz |
| Internal Calibration: | Automatic based on Natural K, U, and T |
| Field of View (FOV): | 45 Degrees |
| Cross Field Scan Coverage: | 300 meters @ 300-meter collection altitude (AGL) |
| Altitude Determination: | 2.4 GHz Radar Altimeter, 10 Meter DEM Database |
| Power: | 28 vdc @ 4 amps full load (3 Packs) |
| Weight: | 136 Kg (300 lbs.) |
| Spin-up Time: | Less than 5 minutes |
| Standard Outputs: | 1024 Gamma Ray Spectra, GPS (2 Hz) |
| Data Processing | 1 Step Full Processing of Total Count, Sigma, and Exposure Rate, approximately 1 minute processing time after data collection. |

D. Radiological Data Processing

All radiological data is processed automatically using airborne algorithms. Normally, a specifically designed survey flight path is flown by the aircraft and once complete, a suite of radiological products is generated from the collected data. Since radiological sources are universally present from the earth and from cosmic sources, all radiological data must be corrected to establish a baseline measurement. Cosmic estimates are established by flying the aircraft 3000 feet AGL while collecting gamma spectral data. At altitudes of 3000 feet and greater all radiological inputs are either from the cosmic sources or the aircraft (which is a constant). Quantified cosmic contributions are stripped out from all subsequent data. Depending on the length of the radiological survey, cosmic backgrounds may be collected at the beginning and end of the survey. In a fashion like the cosmic correction, the natural radiological background for the survey area is also established. This process normally calls for collecting a limited amount of data (a test line) at

the survey altitude (300 – 500 ft. AGL) in an area of similar geology/land use but outside of the region of survey interest. By subtracting the test line data from the survey data, a corrected radiation map for the survey area is generated.

Several data products are generated automatically by the system including total counts, a sigma map, and an exposure map. The total count product is generated by mapping the corrected total count data (approximately 30 – 3000 KeV) from the spectrometers using the integrated GPS data as the geographic datum. Exposure Rate mps are normally contoured at regular intervals in micro-Roentgens (μR). Figure 18 illustrates a typical survey total count plot.

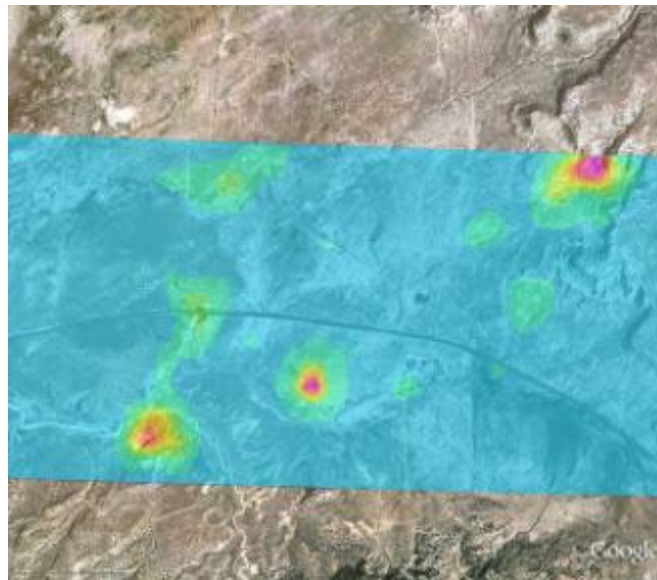


FIGURE 17 - Total Count Plot

A second radiological product includes an array of isotope specific sigma plots or maps. These plots are very useful to the first responder since they help highlight specific data points that may require detailed ground investigation. This procedure consists of a two-step method with the first being a windowing for selected isotope energies followed by a statistical treatment of the data. Isotope specific data is generated by windowing the gamma spectrum at energy levels corresponding to the isotopes of interest. As part of this

analysis, higher energy contributions from uranium and thorium are removed using a stripping coefficient. A statistical average and standard deviation are next computed for the entire survey area using the isotope windowed data. Since the standard deviation provides a measure of the variance of the data set, data values showing several standard deviations (sigma) indicate that these values are statistically different from much of the population. ASPECT uses a graded scale in which 0 to 4 sigma are considered normal and greater than 4 sigma highlights data very different from the population. Greater than 6 sigma indicates that the data is extremely different and warrants additional investigation. By using different isotope windows, several sigma maps can be generated for a given survey (Figure 18).

The final set of products generated by the gamma ray spectrometers consist of an exposure plot or map. This procedure consists of extrapolating the measured total count data collected at the flight altitude down to the total count that would be measured 1 meter above the surface. This method utilizes a weighting algorithm that provides more focus on the high energy counts since these represent the most energetic and penetrating gamma rays. The extrapolation process is accomplished using the calibration coefficients developed as part of the exterior calibration process. The resulting data is plotted in $\mu\text{R/hr}$ and provides the first responder with a health-based estimate of radiological dosage at the ground surface (Figure 19).

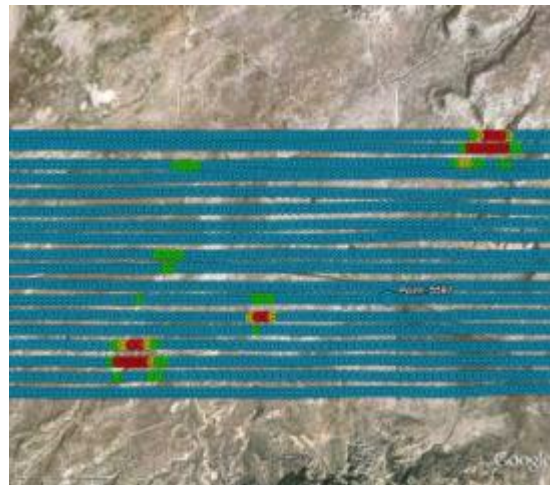


FIGURE 18 - Sigma Plot

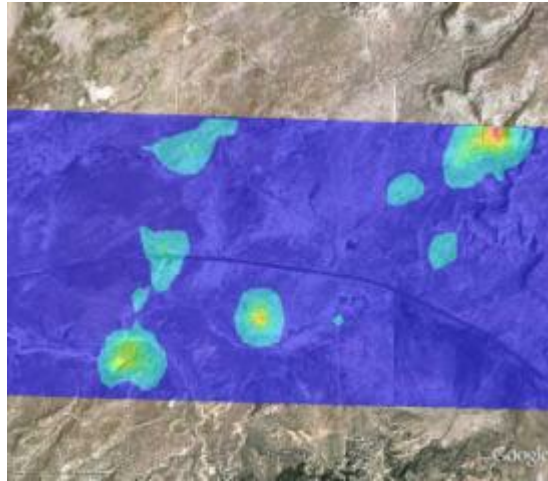


FIGURE 19 - Exposure Plot

4. Aerial Camera Systems

ASPECT utilizes a still digital Imperx camera to collect and provide visible aerial imagery as part of the core data product package (Figure 20 and 21). The system a 28 mm wide-angle lens and is slaved to the primary IR sensors and provides concurrent image collection when the other sensors are triggered for operation. All imagery is geo-rectified using both aircraft attitude correction (pitch, yaw, and roll) and GPS positional information. Imagery can be processed while the aircraft is in flight status or approximately 600 frames per hour can be automatically batch processed once the data is downloaded from the aircraft.

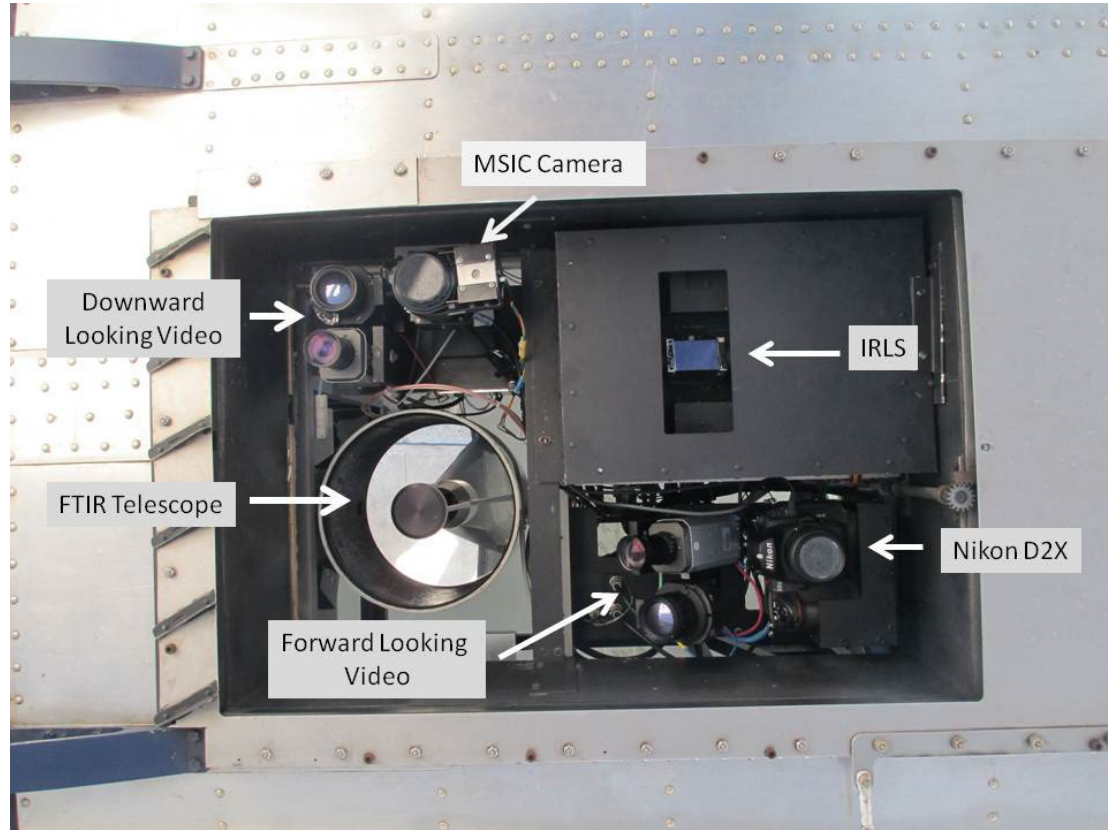


Figure 20: ASPECT Camera Suite



Figure 21 – Imperx Mapping Camera

TABLE 9 - Imperx Aerial Digital Camera Technical Specifications

| | |
|------------------------------------------|---------------------------------------------------------------------------------------------------------|
| System: | Imperx B6640 body |
| Detectors: | 29-megapixel digital CCD sensor (KAI-29050) |
| Aspect Ratio: | 4:5 |
| Lens: | 24 mm Digital Compatible |
| Field of View (FOV): | 824 meters Cross flight and 548 meters Direction of Flight @ 850-meter collection altitude (AGL) |
| Pixel Resolution (IFOV): | 92 cm @ 850-meter collection altitude (AGL) |
| Frame Timing and Collection Rate: | Operator Selectable, 1 to 15 seconds, approximately 600 frames per hour for normal mission |
| Trigger Control: | Automatic, Manual, and Slave |
| Power: | 12 vdc @ 1-amp full load |
| Spin-up Time: | Less than 2 minutes from System Start |
| Standard Outputs: | JPEG, TrueSense |
| Data Processing: | Full INS/GPS Geospatial Rectification |

A. Canon EOS Oblique Camera

To provide situational information from the perspective of the flight crew, ASPECT also supports an oblique camera system that is operated from the right side of the aircraft. This camera consists of a Canon EOS Rebel digital SLR camera body with a 30 – 120 mm

variable zoom lens (Figure 22). Frames are collected at an approximate the 2 o'clock position relative to the aircraft with the target approximately 1000 meters from the aircraft. Figure 23 provides examples of an aerial (downward view) photo and an oblique (side view) photo. The aerial photos are taken at an altitude of about 2,800 feet above the ground (AGL) and the oblique photos are taken at lower altitudes ranging from 500 feet to about 1,200 feet AGL. Table 10 provides technical specification of the oblique camera system.



Figure 22 - Canon EOS Rebel Digital SLR Camera

TABLE 10 - Canon EOS Aerial Oblique Digital Camera Technical Specifications

| | |
|--------------------------|-------------------------------------------|
| System: | Canon EOS Camera Body |
| Detectors: | 6.3-megapixel digital CMOS sensor |
| Aspect Ratio: | 3:5 |
| Lens: | 30-120 mm zoom, Digital Compatible |
| Trigger Control: | Manual |
| Power: | Internal Battery |
| Standard Outputs: | JPEG, Tiff |
| Data Processing: | Spatial Geo-reference |

B. Visible Imagery Data Processing

Visible imagery collected with the ASPECT System is ultimately processed into a geo-registered jpeg or tiff format image. Image processing is composed of two primary steps including image enhancement and geo-registration. Both processing steps can be processed while the aircraft is in flight status but typically, imagery is processed once the aircraft lands due to the large quantity of data involved with aerial photography. A standard flight mission often generates 600 aerial images.

The ASPECT aerial camera consists of a still frame 3x4 ratio digital camera. A wide field of view lens is utilized to match the ground width coverage of the line scanner system. Due to the speed of the aircraft and the fact that ASPECT may fly in low light conditions, the camera uses a fixed focus and shutter speed configuration. Raw imagery is subsequently processed to balance contrast and saturation of each image. In addition, since a wide-angle lens is used, edge distortion is corrected using a custom-built camera model. Both overall algorithms are executed automatically in a batch processing system.

The ASPECT camera is fix-mounted to the primary optical base plate. The camera axis is bore sighted to within 0.5 degrees to the axis centers of the other optical systems. While images are being collected, a concurrent system collects both GPS data and inertial data to provide a high-resolution pitch, roll, and yaw correction dataset. An automatic software package merges these data set and geo-corrects each image using a triangular correction mode. The resulting images statistically show less than 11 meters of center frame positional error and less than 1 degree of rotational error. As with the frame enhancement processing, geo-registration is accomplished in a batch mode at a rate of approximately 800 images per hour. Following registration, images can be directly used by the responder or further corrected with minor positional and rotation corrections (Figure 23).

If requested by the data user, aerial photography (and IR imagery) can be stitched into a wide area mosaic. While this process does take some time, a 4 square kilometer mosaic image (approximately 8 frames) can be assembled in about 2 hours (Figure 24).

Oblique digital photography is processed to capture the situational environment from the perspective of the flight crew. All frames are collected from the right side of the aircraft at approximately 45 degrees from the nose of the aircraft. During automated processing, GPS data is used to provide the position that the frame was collected and the direction that the frame was collected is determined from the track of the aircraft and the relative direction that the camera was operated from within the aircraft. Figure 25 illustrates an example of an oblique image.



FIGURE 23 - Digital Aerial Visible Imagery

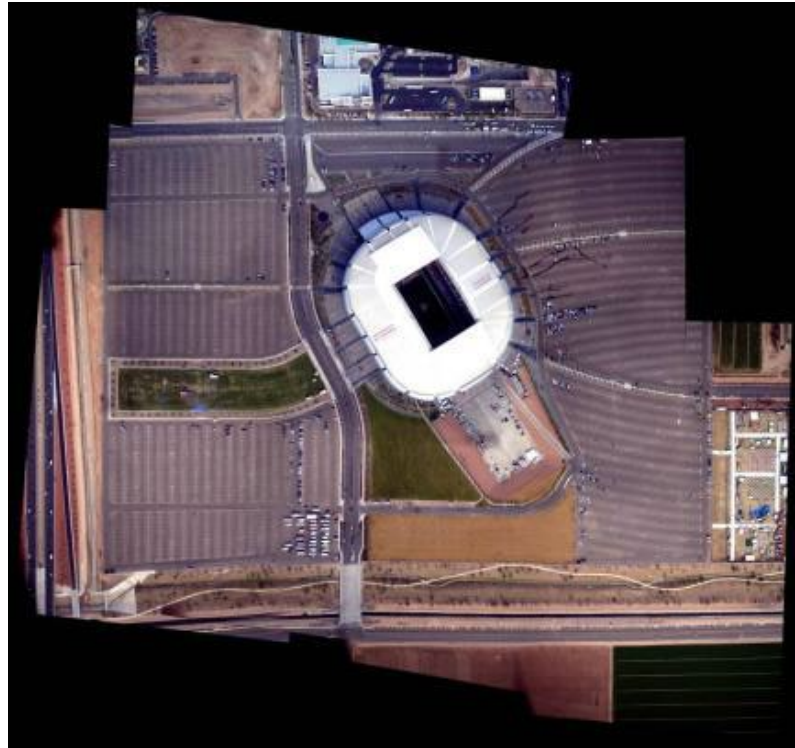


FIGURE 24 - Mosaic Imagery Product



FIGURE 25 - Oblique Aerial Image

C. Data Communication Technology

The ability to rapidly transfer data from the ASPECT aircraft to the ultimate end user is mandatory if the system is to support emergency response functions. ASPECT uses a state-of-the-art satellite-based communication system that provides broadband data through put while the aircraft is in flight status (Figure 26). The system consists of an electronically steered phase array satellite antenna coupled to a RF power amplifier/receiver supporting a wired onboard computer TCP/IP modem/network. All components of the system have been installed and certified as part of a formal FAA STC procedure. The system utilizes a geosynchronous satellite connection and permits full rate communication throughout the contiguous U.S. Table 11 contains the technical specifications for the satellite communications system.



FIGURE 26 - Satellite Communication System Phased Array Antenna

TABLE 11 - Satellite Communication Technical Specifications

| | |
|----------------------------|---------------------------------------------------------------------------------------------------------|
| System: | Chelton Broadband Satellite System |
| Antenna: | HGA-7000 Electronically Steered Phased Array Antenna. |
| Modem: | Integrated Airborne Modem/Router, 100 MB/s data rate |
| Power Amplifier: | HPA-7400 Bi-directional Power Amplifier/Pre-Amplifier Short Coupled to the Phased Array Antenna. |
| Data Rate: | Up to 332 Kbs (Approximately 60 Kbs) Full Duplex |
| Constellation Type: | Fixed Geo-Synchronous |
| Coverage: | Continuous Coverage Over the Lower 48 States. |
| Certification: | FAA STC |
| Power: | 28 vdc @ 10-amp full load |
| Spin-up Time: | Less than 2 minutes from System Start |
| Standards: | TCP/IP |